


RESEARCH

Open Access



Intranasal delivery of PEA-producing *Lactobacillus paracasei* F19 alleviates SARS-CoV-2 spike protein-induced lung injury in mice

Alessandro Del Re^{1*} , Silvia Basili Franzin¹, Jie Lu^{2,3}, Irene Palenca¹, Aurora Zilli¹, Federico Pepi⁴, Anna Troiani⁴, Luisa Seguela¹, Marcella Pesce⁵, Giovanni Esposito^{3,6}, Giovanni Sarnelli^{3,6} and Giuseppe Esposito^{1,3}

Abstract

Background SARS-CoV-2 belongs to the *coronaviridae* family and infects human cells by directly interacting with the angiotensin-converting enzyme-2 (ACE-2) through the viral Spike Protein (SP). While vaccines are crucial, much attention has been directed towards managing the symptoms of acute respiratory distress syndrome. Our present study highlights the potential in counteracting lung inflammation triggered by SARS-CoV-2 SP of the intranasal administration of the engineered probiotic *Lactobacillus paracasei* F19 expressing the enzyme NAPE-PLD (pNAPE-LP) able to in situ release palmitoylethanolamide (PEA) under a super-low boost of palmitate.

Methods C57BL/6J mice undergo prophylactic treatment with intranasal pNAPE-LP/palmitate for 7 days before a 7 days challenge with intranasal SARS-CoV-2 SP. Then the capability of pNAPE-LP of colonizing the lungs and actively release PEA in situ have been determined by immunofluorescence, western blot and HPLC-MS. Moreover, the innate immune system downregulation and the histological damage rescue exerted by pNAPE-LP have been tested by immunofluorescence, hematoxylin and eosin staining, western blot analysis and ELISA test for the release of the pro-inflammatory mediators.

Results pNAPE-LP effectively colonizes mice lungs and releases the anti-inflammatory compound PEA. Moreover, pNAPE-LP exhibits a protective effect on alveolar morphology, innate immune cells infiltration and in the reduction of neutrophil count, effectively reducing lung injury induced by SARS-CoV-2 SP. This is achieved by mitigating TLR4-mediated NLRP3 activation and the downstream pro-inflammatory products such as ILs, TNF α , C-reactive protein and the myeloperoxidase activity. Interestingly we observed a global reduction ACE2 expression in the lungs.

Conclusion pNAPE-LP actively protect from severe inflammatory-related symptoms in SP-challenged mice. Also, it can downregulate the expression of ACE-2 receptors at the lung site potentially preventing the spreading of the infection.

Keywords Engineered probiotic, Palmitoylethanolamide, SARS-CoV-2, Spike protein, ARDS, NLRP3

*Correspondence:
Alessandro Del Re
alessandro.delre@uniroma1.it

Full list of author information is available at the end of the article



Background

Over the past two decades, there has been a concerning surge in the emergence of novel viral diseases [1] and lastly the world has been grappling with the SARS-CoV-2 pandemic, resulting in nearly 7 million deaths to date [2]. SARS-CoV-2 is classified within the *coronaviridae* family and engages human cells through a direct interaction with the angiotensin-converting enzyme-2 (ACE-2) via the viral Spike Protein (SP). This infection precipitates a range of symptoms, notably including acute respiratory distress syndrome (ARDS) and multiorgan failure in the worst-case scenario [3].

Despite the conclusion of the crisis and the gradual global reversion to a state of normalcy, numerous scholarly investigations are underscored by the prospect that COVID-19 possesses the capacity to transmute its epidemiological characteristics from a pandemic manifestation into an endemic counterpart [4], thereby undergoing a change into a seasonal infection. Moreover, taking into account the the impending threat of future pandemics [5], coupled with the fact that recent viral diseases predominantly propagate via airborne transmission, an imperative and pressing demand arises for efficacious preventative interventions.

While vaccines were effectively preventing the worst clinical outcomes of the COVID-19 [6], the possible emergence of new variants of concern as well as the possibility of new airborne outbreaks, much attention has been directed towards managing ARDS. This condition occurs when macrophages and mast cells fail to regulate the innate immune response [7, 8], leading to an excessive release of pro-inflammatory mediators furtherly amplified by the activation of the Nod-like receptor family pyrin domain containing 3 (NLRP3) inflammasome [9–12]. It appears that the SP of SARS-CoV-2 triggers this hyper-inflammatory response by interacting with the Toll-like receptor 4 (TLR4) and triggering a sort of bacterial-like response in the innate immune system [13–15]. Extensive research has demonstrated the direct association between these components, which plays a pivotal role in ARDS development and various short-term and long-term manifestations of COVID-19 [16, 17]. Furthermore, TLR4-related pathways may enhance viral infectivity by indirectly upregulating the ACE-2 receptor in different cell subtypes during inflammatory conditions [18–20].

Recent scientific studies have shed light on autacoid local injury amides (ALIAmides), a class of naturally occurring molecules synthesized by the N-acyl phosphatidylethanolamine-specific phospholipase D (NAPE PLD) in response to specific demands. ALIAmides are promising valuable tool in the clinical management of COVID-19 and other viral diseases by acting on peroxisome proliferator-activated receptors (PPARs) and reducing

the inflammatory response [21–23]. They achieve this by downregulating the expression of several pro-inflammatory mediators and cytokines, including interleukin (IL)-6 and IL-1 β . Additionally, ALIAmides can decrease the expression of TLR4 and NLRP3, both of which are involved in the development of ARDS [24–26].

Our research group recently demonstrated that palmitoylethanolamide (PEA), a specific type of ALIAmide, can effectively reduce in vitro the expression of ACE-2 in alveolar macrophages activated by the SP of SARS-CoV-2 (see Fig. 1 for a summary of our previous findings) [18]. Notably, clinical trials have shown the clinical efficacy and safety of PEA in treating other viral lung diseases such as influenza and the common cold [27]. Currently, PEA is the subject of two clinical trials in Italy and the United States, assessing its effectiveness in managing COVID-19-related symptoms [28, 29].

However, the clinical utility of PEA is limited by its low solubility and the consequent need of using high doses to attain and maintain the therapeutic effect, underscoring the importance of localizing the release of PEA to enhance regional absorption [30]. To enhance its local bioavailability, our laboratory developed a modified strain of *Lactobacillus paracasei subsp. paracasei F19* carrying a plasmid that expresses the NAPE-PLD enzyme (pNAPE-LP). By releasing PEA under a super-low boost of palmitate, this probiotic system has already demonstrated effectiveness in reducing inflammation in the gut across various colitis models. In these previous investigation we observed an *optimum* of PEA production at the palmitate concentration of 0.003 μ M [31, 32]. Moreover, considering the established connection between lung microbiota disruption and ARDS, pNAPE-LP holds promise as a prophylactic agent against ARDS by mitigating inflammatory responses also by restoring lung microbiota [33, 34]. Finally, its local action makes it a compelling candidate for intranasal delivery. Therefore, the objective of this study is to investigate the prophylactic anti-inflammatory effect of intranasal administration of the pNAPE-LP system combined with palmitate in a SARS-CoV-2 SP-induced lung injury model. Initially, we confirmed the ability of pNAPE-LP to colonize the lungs and release PEA in situ. Subsequently, through histological, immunofluorescence, Western blot, and ELISA analyses, we assessed the ability of our probiotic system to preserve alveolar architecture integrity and reduce the increase of pro-inflammatory markers (NLRP3, TLR4, etc.).

Materials and methods

Generation of genetically modified strains of *Lactobacillus paracasei subsp. paracasei F19*

The pTRKH3-slpGFP vector obtained from Addgene (Watertown, MA, USA) underwent several

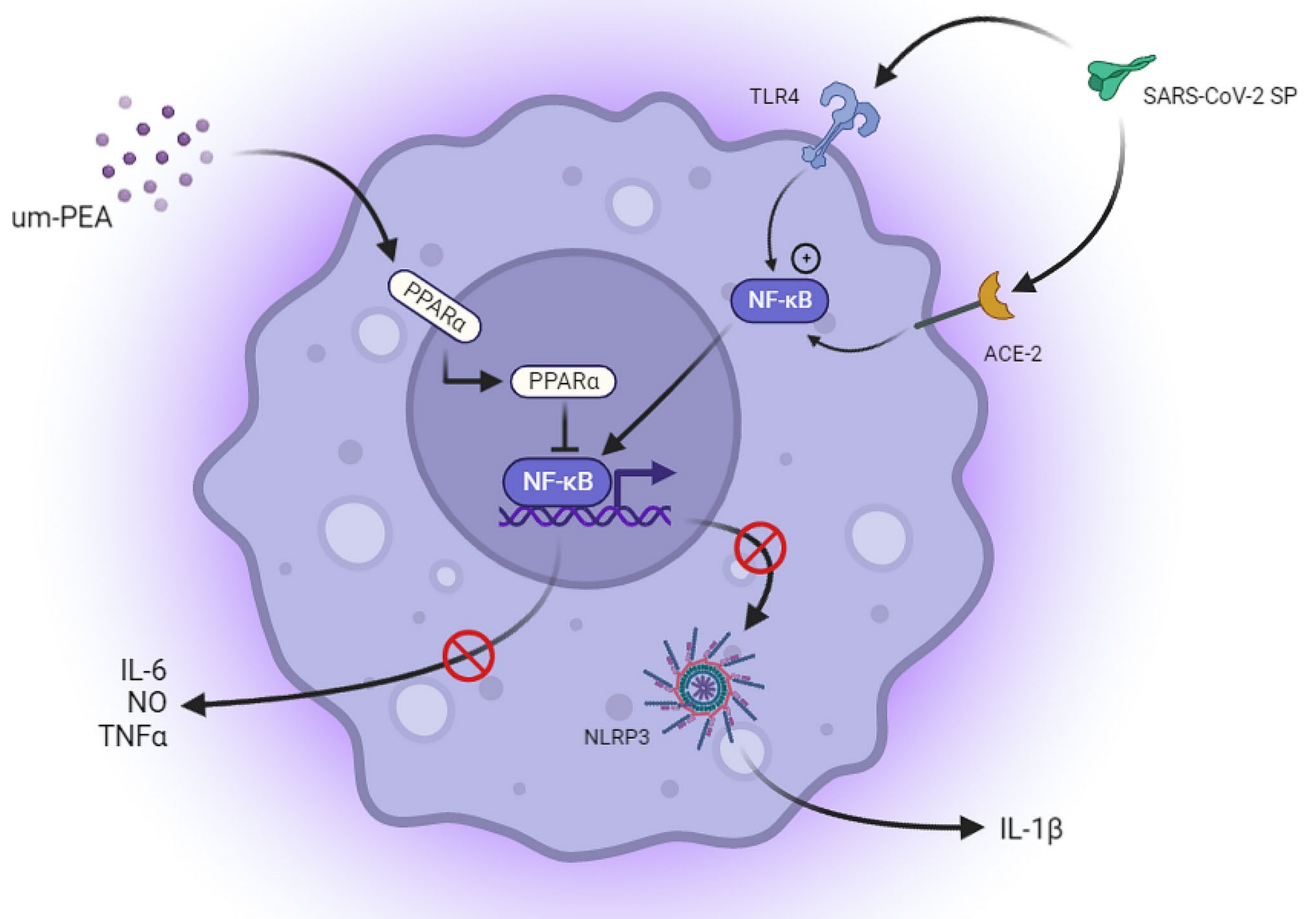


Fig. 1 Summary of previous findings. Effect of ultramicrosized (um)-PEA on SP-challenged murine alveolar macrophages. Anti-inflammatory effect of um-PEA in SARS-CoV-2 spike protein challenged murine alveolar macrophages depends upon PPAR α -mediated control of NF- κ B and NLRP3 inflammasome signaling pathways. Schematic representation of SARS-CoV-2 spike protein-induced inflammation and relative proposed anti-inflammatory mechanism of um-PEA in mice alveolar macrophages. Spike protein interacts at TLR4 and ACE-2 receptor sites, activating phosphorylation of p38MAPK and consequent NF- κ B activation. This is accompanied by cytokine release (IL-6 and TNF- α) and inflammasome pathway activation, featured by NLRP3 and Caspase-1/IL-1 β upregulation. Um-PEA acting at PPAR- α receptor site inhibits NF- κ B transcription and NLRP-3 inflammasome signaling leading to a significant anti-inflammatory effect in spike protein-challenged alveolar macrophages

modifications. Firstly, the GFP sequence was eliminated at Sall/PstI restriction sites, followed by the insertion of T7 transcriptional terminators at BamHI/EcoRV sites, and finally, linker sequences containing BsaI-BsaI were added at PstI/XmaI restriction sites. Then, using the In-Fusion method (Clontech, Mountain View, CA, USA), the cDNA of human NAPE-PLD was inserted into the BsaI sites. Electroporation was used to transfect the resulting pTRKH3-slp-NAPE-PLD construct and the parental plasmid (which does not express the NAPE-PLD gene and is used as a negative control) into *Lactobacillus paracasei subsp. paracasei* F19 strain (Arla Foods, Hoersholm, Denmark). Positive clones were obtained by erythromycin (5 μ g/mL) selection. The parental plasmid (pLP) and NAPE-PLD-expressing bacteria (pNAPE-LP) were then anaerobically amplified in Man, Rogosa and Sharpe (MRS)-broth (Conda, Torrej3n de Ardoz Madrid,

Spain) and isolated in MRS agar (Conda, Torrej3n de Ardoz Madrid, Spain) supplemented with erythromycin 5 μ g/mL (Sigma-Aldrich, Milan, Italy) under anaerobic conditions at 37 $^{\circ}$ C for 72 h. Finally, the viability of the bacteria was determined by manually counting colonies, and the colony forming units (CFU)/mL were obtained by correcting the number of colonies for the dilution factor.

Animals and experimental plan

Eight-week-old male C57BL/6J mice (Charles River, Lecco, Italy) were used for the experiments. Sapienza University's Ethics Committee approved all experimental procedures. Animal care was in compliance with the IASP and European Community (EC L358/1 18/12/86) guidelines on the use and protection of animals in

experimental research. The Experimental plans last for 14 days in total (from day -7 to day 7, see Fig. 2).

For the intranasal administration the animals were lightly anesthetized by inhaled isoflurane (Abbott Laboratories, Montreal, PQ, Canada), and 2 or 4 volumes (25 μ l each) of bacterial suspensions, SP solution, Palmitate solution or vehicle were intranasally delivered dropwise to the nares using a pipetman (model P20 or P200, Gilson) while the mouse was in a supine position. In details, the animals were randomly divided into 5 groups $n=8$ each and undergo treatments as follow: (1) Vehicle, daily intranasal administration of sterile saline solution along the entire experimental plan; (2) SARS-CoV-2 SP 500 μ g/Kg, daily intranasal administration of sterile saline solution from day -7 to -1 and daily intranasal administration of SP 500 μ g/Kg from day 1 to day 7; (3) pNAPE-LP/Palmitate 0.003 μ M, daily intranasal administration of 10^9 CFU of pNAPE-LP+Palmitate 0.003 μ M from day -7 to day -1 and daily intranasal administration of SP 500 μ g/Kg from day 1 to day 7; (4) pLP/Palmitate 0.003 μ M, daily intranasal administration of 10^9 CFU of pLP+Palmitate 0.003 μ M from day -7 to day -1 and daily intranasal administration of SP 500 μ g/Kg from day 1 to day 7; (5) Palmitate 0.003 μ M, daily intranasal administration of Palmitate 0.003 μ M from day -7 to day -1 and daily intranasal administration of SP 500 μ g/Kg from day 1 to day 7. All the solutions for the intranasal inoculation have been prepared in sterile saline as described in the Supplementary Table 1. Rectal temperature was measured daily for the entire duration of the experiment. To obtain the rectal temperature, the

mice were hand-restrained and placed on a horizontal surface. The tail was then lifted, and the probe (covered with Vaseline) was gently inserted into the rectum, up to a fixed depth. At day 7 the animals were sacrificed by CO_2 hypoxia.

Sample collection and preparation

Broncho-alveolar lavage fluid (BALF) was collected in the following manner. The mice were dissected to expose the trachea, and a small incision was made. A sterile tube (with an internal diameter of 0.58 mm) was inserted through the incision and connected to a sterile syringe needle. To create an airtight seal, a piece of sterile surgical thread was tightly wrapped around the intubated trachea. Two rounds of instillation and retrieval of 1 mL of sterile phosphate-buffered saline (PBS) into the lungs were then performed using the sterile syringe. To ensure the integrity of the procedure, the tubing-needle-syringe setup was rinsed thoroughly with sterile PBS between each sample collection. Sterile PBS ($n=2$) was used for lavage, and PBS rinses ($n=4$) of the syringe, needle, and tubing (before and after lavage) were collected as procedural controls. BAL fluid was prepared by pooling the two sequential lavages from each mouse, resulting in up to 2 mL of total BAL fluid per mouse.

To prepare perfused lungs for H&E and immunofluorescence analysis, a solution of 4% PFA was injected directly into the lung through the trachea, which was then secured with a piece of thread. The lungs were subsequently immersed in the same fixative for 24 h. Following fixation, the lungs were perfused and then immersed

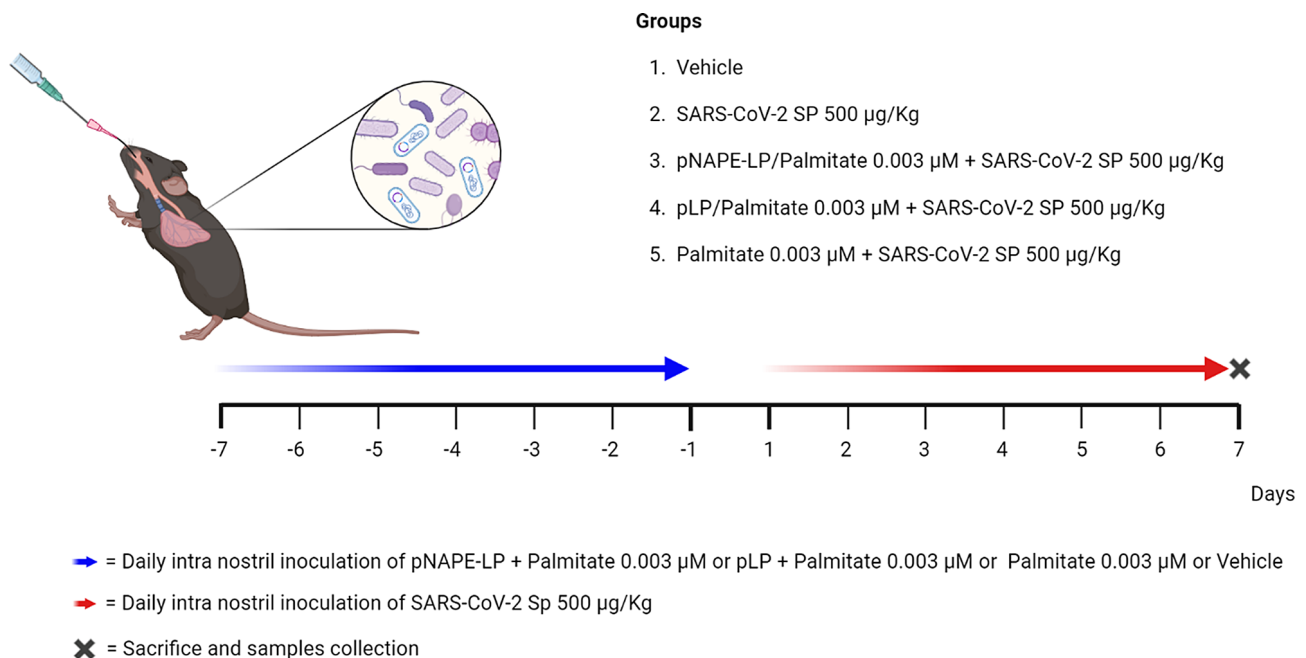


Fig. 2 Experimental plan

in 30% sucrose for 24 h. Finally, the lungs perfused and immersed in OCT for a period of 24 h before the cryostat cutting.

Lungs homogenates were obtained from non-PFA fixed lungs. The snap-frozen lungs were thawed, weighed, transferred to different tubes on ice containing hypotonic lysis buffer (10 mM 4-(2-hydroxyethyl)-1-piperazineethanesulfonic acid (HEPES), 1.5 mM MgCl₂, 10 mM KCl, 0.5 mM phenylmethylsulphonylfluoride, 1.5 mg/mL soybean trypsin inhibitor, 7 mg/mL pepstatinA, 5 mg/mL leupeptin, 0.1 mM benzamidine and 0.5 mM dithiothreitol (DTT)). The samples were centrifuged at 10,000 × g for 10 min and supernatants were transferred to clean microcentrifuge tubes, frozen on dry ice and stored at -80 for the analysis.

Confirmation of pNAPE-LP lung colonization

BALF collected from groups 1 and 3 as previously described were immediately diluted in serial 1/10 dilutions (from 10⁻¹ to 10⁻⁵) and plated in MRS agar enriched with Erythromycin [50 µg/mL] as selection marker. The plates were incubated for 72 h at 37 °C in a microaerophilic environment and then the colonies from each spot were counted to determine the CFU/mL contained in the BALF samples. *N*=4 single colonies have been picked up from the 10⁻⁵ dilution and inoculated in MRS liquid media enriched with Erythromycin [50 µg/mL] and growth overnight. According to the procedure previously described [17] with slight modifications, immunofluorescence analysis was performed in both pNAPE-LP and in the cultured pLP as a negative control. Briefly, the cultures undergo spinning and the pellets were washed in phosphate buffer saline (PBS). For immunofluorescence staining of both pNAPE-LP and in the pLP, 1×10⁷ bacterial cells were placed on polyethylenimine-coated coverslips and fixed with 4% PFA. Blocking solution containing 1% bovine serum albumin (BSA) in PBS (w/v) was used. Labelling was performed using polyclonal rabbit anti-NAPE-PLD antibody (1:100 dil. v/v) (Cell Signaling Technology, Inc., Danvers, MA, USA). Secondary fluorescein isothiocyanate-conjugated anti-rabbit antibodies were incubated at room temperature for 2 h in the dark. Samples were examined by Optika XDS-3L4 microscope (Ponteranica, Bergamo, Italy). Images were captured at 100× by a high-resolution digital camera (Nikon Digital Sight DS-U1).

HPLC-MS determination of PEA level in mice lungs

Specimens from the lung from every groups of mice were isolated to evaluate PEA concentrations in vivo. Tissues were processed according to the method described by the Endocannabinoid Research Group [39]. Extraction and analysis were performed according to Gachet et al. [40], with slight modifications.

Analyses were run on a Jasco Extrema LC-4000 system (Jasco Inc., Easton, MD, USA) coupled to an Advion Expression mass spectrometer (Advion Inc., Ithaca, NY, USA) equipped with an electrospray (ESI) source. Mass spectra were recorded in positive SIM mode. The capillary voltage was set at +180 V, the spray voltage was at 3 kV, the source voltage offset was at +20 V, and the capillary temperature was set at 250 °C. The chromatographic separation was performed on a Kinetex C18 analytical column (150×4.6 mm, id. 3 µm, 100 Å) and security guard column, both supplied by Phenomenex (Torrance, CA, USA). The analyses were performed at a flow rate of 0.3 mL/min, with solvent A (water containing 2 mM ammonium acetate) and solvent B (methanol containing 2 mM ammonium acetate and 0.1% formic acid). Elution was performed according to the following linear gradient: 15% B for 0.5 min, 15–70% B from 0.5 to 2.5 min, 7–99% B from 2.5 to 4.0 min and held at 99% B from 4.0 to 8.0 min. From 8 to 11.50 min, the column was equilibrated to 15% B and conditioned from 11.5 to 15.0 min at 15% B. The injection volume was 10 µL and the column temperature was fixed at 40 °C. For quantitative analysis, standard curves of PEA (Sigma-Aldrich St. Louis, MO, USA) were prepared over a concentration range of 0.0001–1 ppm with six different concentration levels and duplicate injections at each level. All data were collected and processed using JASCO ChromNAV (v2.02.04) and Advion Data Express (v4.0.13.8).

Western blot analysis

Proteins were extracted from lung tissue or bacteria pellets and processed by Western blot analysis. For protein extraction by the bacterial pellet, a specific CellLytic™ lysis buffer (Sigma-Aldrich, Milan, Italy) was used according to manufacturer's instructions. Tissue samples were homogenized in ice-cold hypotonic lysis buffer [10 mM 4-(2-hydroxyethyl)-1-piperazineethanesulfonic acid (HEPES), 1.5 mM MgCl₂, 10 mM KCl, 0.5 mM phenylmethylsulphonylfluoride, 1.5 µg/ml soybean trypsin inhibitor, 7 mg/ml pepstatin A, 5 mg/ml leupeptin, 0.1 mM benzamidine, and 0.5 mM dithiothreitol (DTT)]. Both bacterial- and tissue-deriving protein extracts were mixed with a non-reducing gel loading buffer [50 mM Tris (hydroxymethyl)aminomethane (Tris), 10% sodium dodecyl sulfate (SDS), 10% glycerol, 2 mg/ml bromophenol] at a 1:1 ratio, and then boiled for 3 min followed by centrifugation at 10,000×g for 10 min. The protein concentration was determined using Bradford assay and equivalent amounts (50 µg) of each homogenate underwent electrophoresis through a polyacrilamide minigel. After the transfer the membranes were incubated with 10% nonfat dry milk in

Table 1 Antibodies for western blot

Antibody	Host	Clonality	Dilution	Brand
Anti-NLRP3	Rabbit	Monoclonal	1:100 v/v	Thermo Fisher Scientific, Waltham, MA, USA, Cat #MA5-32255
Anti-cleaved caspase 1	Mouse	Monoclonal	1:100 v/v	Santa Cruz Biotechnology, Dallas, TX, USA, sc-56,036
Anti-NAPE-PLD	Rabbit	Polyclonal	1:200 v/v	AbCam, Cambridge, UK, ab95397
Anti-TLR4	Rabbit	Polyclonal	1:50 v/v	Bioss Antibodies, Boston, MA, USA, bs-1021R

Table 2 Antibodies for immunofluorescence

Antibody	Host	Clonality	Dilution	Brand
Anti-NLRP3	Rabbit	Monoclonal	1:100 v/v	Thermo Fisher Scientific, Waltham, MA, USA, Cat #MA5-32255
Anti-ACE2	Mouse	Monoclonal	1:50 v/v	Santa Cruz Biotechnology, Dallas, TX, USA, sc-390,851
Anti-CD68	Goat	Monoclonal	1:200 v/v	AbCam, Cambridge, UK, ab289671
Anti-TLR4	Rabbit	Polyclonal	1:50 v/v	Bioss Antibodies, Boston, MA, USA, bs-1021R

PBS overnight at 4 °C and then exposed, depending on the experiments, with the appropriate primary antibody according to standard experimental protocols (see Table 1). Membranes were then incubated with the specific secondary antibodies conjugated to HRP (Dako, Milan, Italy). Immune complexes were exposed to enhanced chemiluminescence detection reagents, and the blots were analyzed by scanning densitometry (Versadoc MP4000; Bio-Rad, Segrate, Italy). Results were expressed as optical density (OD; arbitrary units=mm²) and normalized against the expression of the housekeeping proteins β -actin for mice samples and GroEL for bacterial pellets.

Hematoxylin and Eosin (H&E) staining and lung injury assessment

Frozen sections of the lungs were sectioned using a cryostat at 8 μ m and placed onto slides. The sections were stained with H&E according to Ling et al. [35]. The histopathological analysis has been performed in the following manner. Number of epithelial cells, and the number infiltrated neutrophils in alveolar spaces and interstitial space were analyzed by NIH Image J. Ten 40x fields from each group were chosen for the counting of the epithelial and infiltrated neutrophils. Lung injury score was measured as described by Matus-Bello et al. [36] following a scale (see Supplementary Table 2).

Immunofluorescence

Frozen sections of the lungs were sectioned using a cryostat at 8 μ m and placed onto slides. Sections were blocked with bovine serum albumin (BSA) and subsequently stained with the appropriate primary antibody (See Table 2). Slices were then washed with PBS 1X and incubated in the dark with fluorescein isothiocyanate-conjugated anti-rabbit or anti-mouse (Abcam, Cambridge, UK). Nuclei were stained with Hoechst. Sections were analyzed with a microscope (Nikon Eclipse 80i), and images were captured by a

high-resolution digital camera (Nikon Digital Sight DS-U1).

Myeloperoxidase assay

Myeloperoxidase (MPO), a marker of polymorphonuclear leukocyte accumulation, was determined as previously described (Mullane et al., 1985). After removal, lungs tissues were rinsed with a cold saline solution. Then, the tissues were homogenized in a solution containing 0.5% hexadecyltrimethylammonium bromide (Sigma-Aldrich, Milan, Italy), dissolved in 10 mM potassium phosphate buffer, and centrifuged for 30 min at 20,000 \times g at 37 °C. An aliquot of the supernatant was mixed with a solution of tetramethylbenzidine (1.6 mM; Sigma-Aldrich, Milan, Italy) and 0.1 mM hydrogen peroxide (Sigma-Aldrich, Milan, Italy). The solution was then spectrophotometrically measured at 650 nm. MPO activity was determined as the amount of enzyme degrading 1 mmol/min of peroxide at 37 °C and was expressed in milliunits (mu) per 100 mg of wet tissue weight.

Enzyme-linked immunosorbent assay (ELISA)

ELISA for IL-1 β , IL-6, TNF α and CRP (all from Thermo Fisher Scientific, MA, USA) was carried out on lungs homogenate according to the manufacturer's protocol. Absorbance was measured on a microtiter plate reader. IL-1 β , IL-6, TNF α and CRP levels were determined using standard curve methods.

Results

pNAPE-LP colonizes mice lungs and actively releases PEA in situ

In order to validate the lung colonization by our probiotic system, we cultured the BALF obtained from groups (1) and (3) on MRS agar supplemented with erythromycin [50 μ g/mL]. Our findings revealed the presence of erythromycin-resistant colonies exclusively in the samples derived from the group subjected to intranasal administration of pNAPE-LP (Fig. 3, A). Additionally, the samples from group (3) exhibited an average level of 10⁴

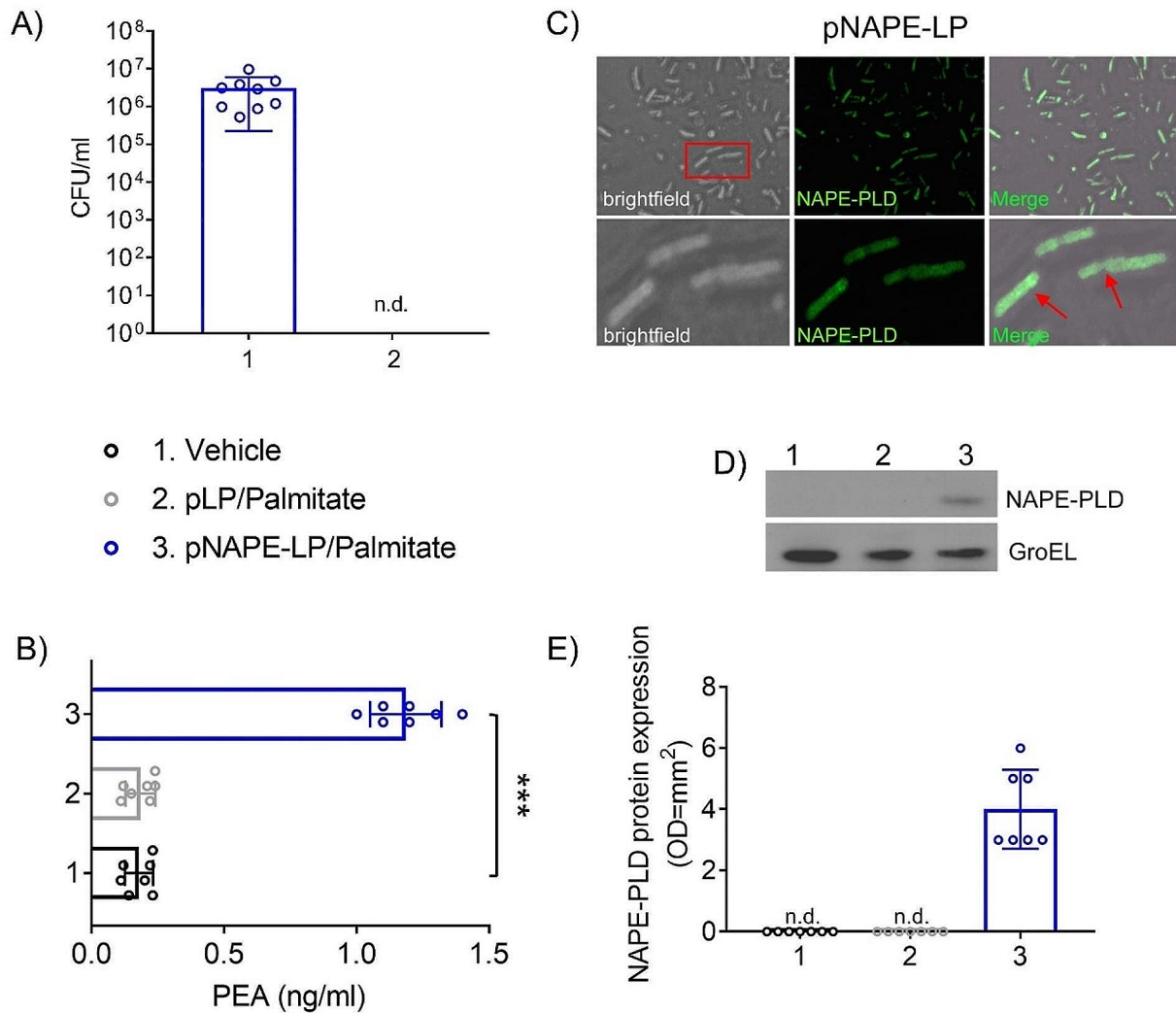


Fig. 3 Confirmation of pNAPE-PLD colonization of the mice lungs. At the end of the experimental protocol the BALF from pNAPE-LP/Palmitate group displays significant levels of erythromycin resistant CFU compared to the Vehicle group (**A**). Once picked and amplified, these cells are revealed to express the NAPE-PLD enzyme as confirmed by immunofluorescence (**C**), and western blot analysis (46 kDa) (housekeeping protein GroEL, 57 kDa) (**D**, **E**). The HPLC-MS analysis of homogenates of lungs revealed a significant increase in the levels of PEA only in pNAPE-LP/Palmitate group (**B**). Results are expressed as mean \pm SD of $n=7$ or 9 experiments performed in triplicate. *** $p < 0.001$, ** $p < 0.01$, * $p < 0.05$ vs. Vehicle, n.d.=non detectable

CFU/mL (Fig. 3, B), thereby confirming the successful colonization of the lungs by pNAPE-LP. To further corroborate our observations, four colonies were selected from each sample and cultured overnight in MRS liquid media supplemented with erythromycin. Subsequently, the resulting cultures underwent Immunofluorescence and western blot analyses to ascertain the expression of the NAPE-PLD enzymes. Our immunofluorescence

analysis (Fig. 3, C) and western blot results (Fig. 3, D-E) demonstrated the selective expression of the NAPE-PLD enzyme exclusively in the bacterial cells isolated from the BALF of group (3).

Moreover, to validate the capacity of pNAPE-LP to locally produce and release PEA under minimal stimulation with palmitate, homogenates of mouse lung samples from groups (1), (3), and (4) were subjected to HPLS-MS

analysis to determine the levels of PEA. Once again, only the samples obtained from animals treated with pNAPE-LP and palmitate exhibited a significant increase in PEA levels ($p < 0.001$ vs. Vehicle group) (Fig. 3, B).

pNAPE-LP protects alveolar morphology and reduces the lung injury score from SARS-CoV-2 SP pro-inflammatory effect

After 7 days of intranasal delivery of SARS-CoV-2 SP, mice in group 2 exhibited a substantial deterioration in

their alveolar architecture, indicating significant damage to the small air sacs in their lungs. In contrast, the prophylactic administration of pNAPE-LP/Palmitate (3) demonstrated a protective effect, effectively preserving the alveolar morphology in the mice's lungs. It is noteworthy that the combination of the engineered probiotic pNAPE-LP and palmitate played a pivotal role in conferring histological protection in our experimental model (Fig. 4, A). The results clearly highlight the efficacy of this

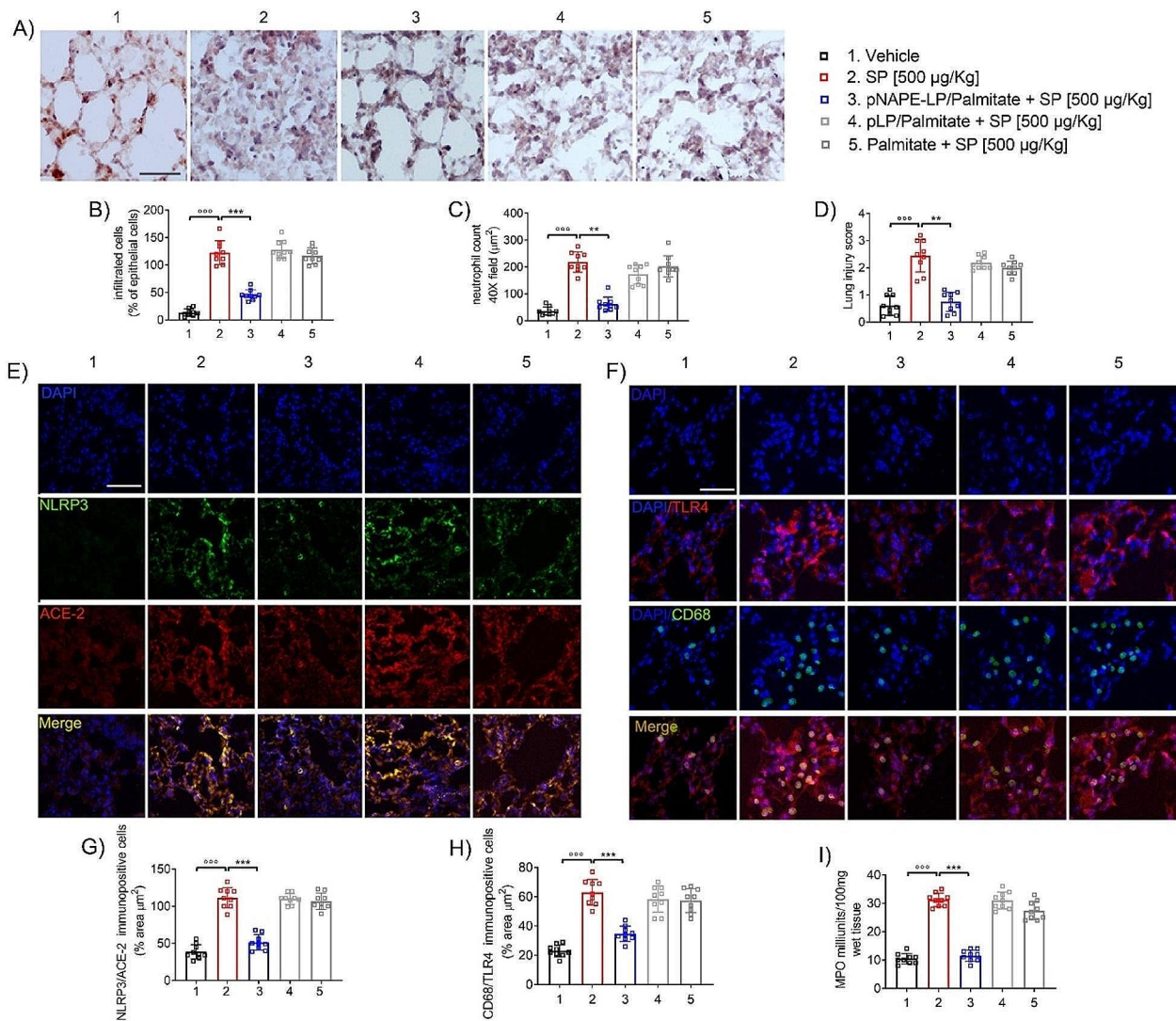


Fig. 4 Prophylactic administration of pNAPE-LP/Palmitate accounts for histological damage attenuation, reduction of pro-inflammatory markers expression and MPO activity in mice lungs. Hematoxylin and eosin (H and E) stained lung specimens (A), relative quantification of infiltrated epithelial cells (B), the neutrophil count (C) and the global lung damage score (D) showing the protective effect of pNAPE-LP/palmitate treatment on SP-induced lung injury (magnification ??X, scale bar: ??? µm). Representative immunofluorescence images showing the co-expression of NLRP3 (green) and ACE-2 (red) and their merge (E) on the left and the expression of TLR4 (red) on the surface of CD68⁺ (green) cells in mice lung specimens with their respective quantification (G,H) display the protective effect of pNAPE-LP/Palmitate treatment on mice lungs following SP-mediated injury. Effect of pNAPE-LP prophylactic treatment in reducing the MPO activity in lung tissue (I). Nuclei were also investigated using DAPI staining. Results are expressed as mean ± SEM of $n = 5$ experiments performed in triplicate. *** $p < 0.001$, ** $p < 0.01$ vs. SP [500 µg/Kg]. Scale bar = 20 µm; magnification 20X

specific combination in mitigating the detrimental effects induced by SARS-CoV-2 SP.

The observed loss of alveolar architecture in group 2 was accompanied by a significant increase in the infiltration of epithelial cells ($p < 0.001$ vs. Vehicle), as well as a marked elevation in the neutrophil count ($p < 0.001$ vs. Vehicle), indicating a pronounced lung injury ($p < 0.001$ vs. Vehicle). However, the prophylactic treatment with pNAPE-LP/Palmitate (3) reversed the histological damage observed in this group. Specifically, it successfully normalized the percentage of infiltrated epithelial cells ($p < 0.001$ vs. SP [500 $\mu\text{g}/\text{Kg}$]), reduced the neutrophil count ($p < 0.01$ vs. SP [500 $\mu\text{g}/\text{Kg}$]), and consequently decreased the overall lung injury score ($p < 0.01$ vs. SP [500 $\mu\text{g}/\text{Kg}$]) to levels comparable to those observed in the vehicle group (Fig. 4, B-D). Consistent with expectations, the two internal control groups, namely pLP/Palmitate (4) and Palmitate alone (5), did not show any significant differences compared to the SP [500 $\mu\text{g}/\text{Kg}$] group (2) in terms of deterioration in their alveolar architecture, the percentage of infiltrated epithelial cells, the neutrophil count and the lung injury score (Fig. 4, A-D).

pNAPE-LP attenuates TLR4-mediated NLRP3 activation in the lungs of mice and reduces global ACE2 expression

To gain insights into the role of SARS-CoV-2 SP agonism on TLR4 *in vivo* and explore the potential protective effect of pNAPE-LP/Palmitate, we conducted immunofluorescent analysis on lung sections of mice. Our objective was to examine the expression of TLR4 in alveolar macrophages (CD68⁺ cells) and its influence on the co-expression of NLRP3 and ACE-2, two important markers of ARDS onset and viral invasion, respectively.

Our findings revealed a significant upregulation of TLR4 in CD68⁺ cells ($p < 0.001$ vs. Vehicle) in samples from the SP [500 $\mu\text{g}/\text{Kg}$] group (2). Similarly, we observed a parallel increase in the co-expression of NLRP3 and ACE-2 ($p < 0.001$ vs. Vehicle) following daily administration of SARS-CoV-2 SP (Fig. 4E-H).

Consistent with previous observations, treatment with pNAPE-LP/Palmitate significantly mitigated the pro-inflammatory environment in the lungs of mice. Notably, the expression levels of TLR4 in CD68⁺ cells were markedly reduced ($p < 0.001$ vs. SP [500 $\mu\text{g}/\text{Kg}$]), as were the overall numbers of CD68⁺ cells, indicating the beneficial effects of the probiotic system compared to the SARS-CoV-2 SP group (2). Similarly, the global co-expression of NLRP3/ACE-2 was significantly diminished by the engineered probiotic ($p < 0.001$ vs. SP [500 $\mu\text{g}/\text{Kg}$]), further confirming its anti-inflammatory properties (Fig. 4E-H).

In contrast, our investigation of the internal control groups, namely pLP/Palmitate (4) and Palmitate alone (5), revealed no significant changes in the expression of the aforementioned markers compared to the SP [500 $\mu\text{g}/$

Kg] group (2). Specifically, there were no notable differences observed in the levels of TLR4 expression in CD68⁺ cells or concerning the co-expression of NLRP3 and ACE-2. These findings suggest that the administration of pLP/Palmitate or Palmitate alone did not exert a significant impact on reducing the expression of these markers when compared to the SP [500 $\mu\text{g}/\text{Kg}$] group (Fig. 4E-H).

pNAPE-LP reduces the MPO activity in mice lungs

To gain a deeper comprehension of the role of innate immunity in SP-induced lung inflammation and to understand the therapeutic potential of pNAPE-LP/Palmitate system, we conducted an MPO assay on samples obtained from all experimental groups.

As anticipated, the SP [500 $\mu\text{g}/\text{Kg}$] group (2) exhibited an elevated MPO activity, indicative of an inflammatory state in the lungs of mice ($p < 0.001$ vs. Vehicle). In contrast, treatment with pNAPE-LP/Palmitate reduced MPO activity to physiological levels ($p < 0.001$ vs. SP [500 $\mu\text{g}/\text{Kg}$]), thereby confirming the probiotic system's ability to restrain over-activation of the innate immune system.

Once again, the internal control groups, pLP/Palmitate (4) and Palmitate alone (5), demonstrated no significant changes in MPO activity levels when compared to the SP [500 $\mu\text{g}/\text{Kg}$] group (2) (Fig. 4, I).

Western blot analysis confirms pNAPE-LP-mediated modulation of NLRP3, TLR4, and caspase 1 expression in SARS-CoV-2 SP-induced lung injury

To further validate the findings obtained from immunofluorescent analysis and delve into the activation of procaspase 1 upon NLRP3 expression, western blot analysis was conducted on lung homogenates.

Corroborating the previous data, our investigation revealed a significant increase in the abundance of TLR4 ($p < 0.001$ vs. Vehicle), NLRP3 ($p < 0.001$ vs. Vehicle), and the cleaved form of caspase1 ($p < 0.001$ vs. Vehicle) in the SP [500 $\mu\text{g}/\text{Kg}$] group (2) when compared to the levels observed in the Vehicle group (1).

Once again, the prophylactic administration of pNAPE-LP/Palmitate demonstrated its ability to reverse this inflammatory trend. It not only reduced the expression of TLR4 ($p < 0.001$ vs. SP [500 $\mu\text{g}/\text{Kg}$]) and NLRP3 ($p < 0.001$ vs. SP [500 $\mu\text{g}/\text{Kg}$]) but also decreased the levels of the effector protein caspase1 ($p < 0.01$ vs. SP [500 $\mu\text{g}/\text{Kg}$]) derived from NLRP3.

In contrast, the internal control groups (4,5) did not exhibit any consistent effect in reducing the levels of the aforementioned proteins. The levels observed in these control groups were comparable to those of the SP [500 $\mu\text{g}/\text{Kg}$] group (2) (Fig. 5, A-D).

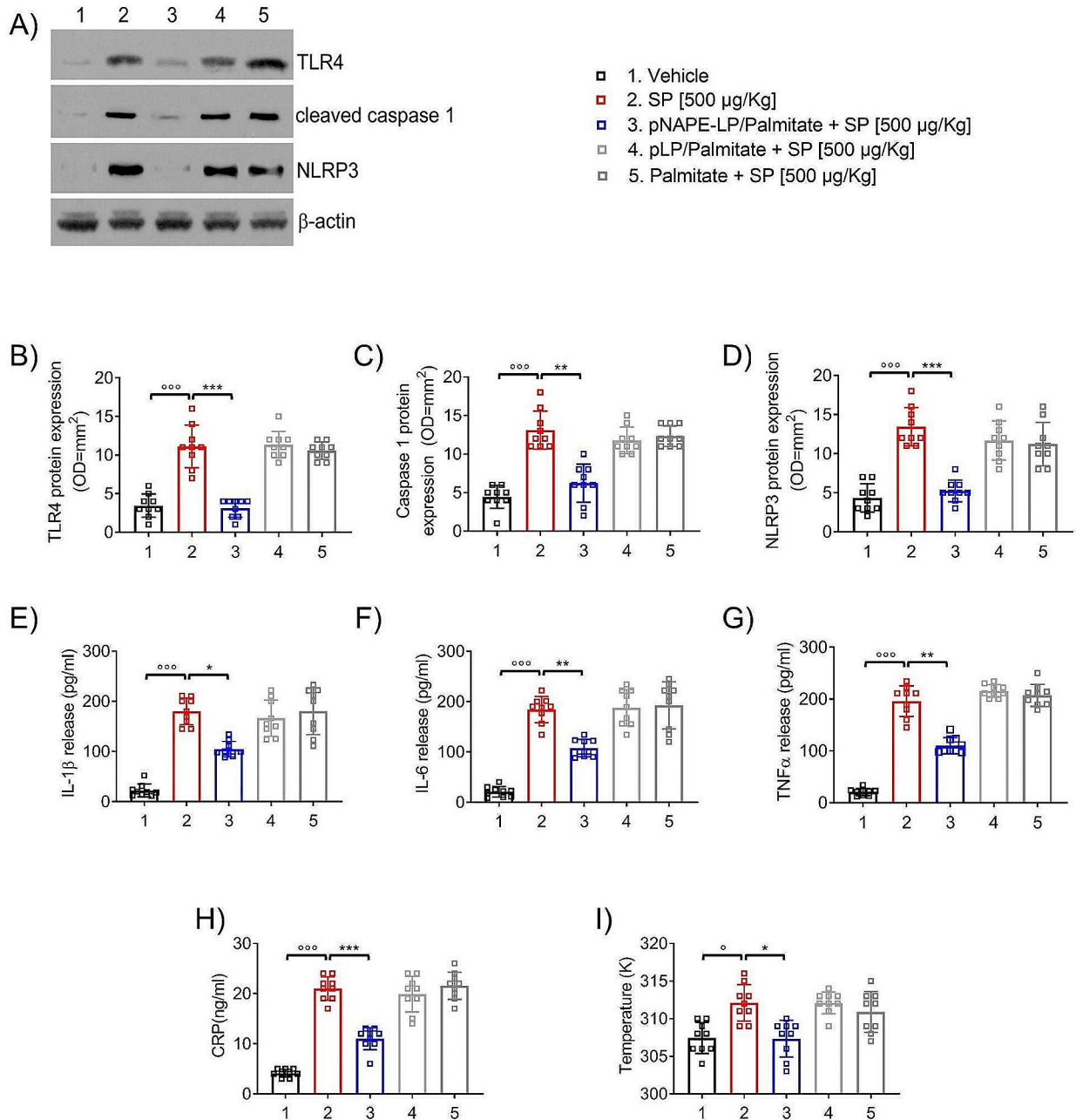


Fig. 5 Prophylactic administration of pNAPE-LP/Palmitate reduces pro-inflammatory markers expression and body temperature in mice. Western blot analysis on lung specimens to detect TLR4 (95 kDa), cleaved Caspase 1 (50 kDa), NLRP3 (120 kDa) and the housekeeping protein β -actin (40 kDa) (**A**), and the relative densitometric quantification (**B**, **C**, **D**) showing the protective effect of pNAPE-LP/palmitate treatment on SP-induced lung injury. pNAPE-LP+palmitate treatment reduces ILs (**E**, **F**), TNF- α (**G**) and CRP (**H**), thus reducing the body temperature (**I**) in SP-challenged mice. Results are expressed as mean \pm SEM of $n=5$ experiments performed in triplicate. *** $p < 0.001$, ** $p < 0.01$, * $p < 0.05$ vs. SP [500 μ g/Kg]

pNAPE-LP/Palmitate treatment reduce the release of IL-1 β , IL-6, TNF α and CRP in the lungs of mice

In conjunction with the western blot analysis, we conducted ELISA tests to assess the levels of downstream effectors released upon activation of the TLR4-NLRP3

pathway in the lungs of mice, including ILs, TNF α and CRP.

Following the same pattern as the previous data, the ELISA test demonstrated a significant increase in the release of IL-1 β ($p < 0.001$ vs. Vehicle), IL-6 ($p < 0.001$ vs.

Vehicle), TNF α ($p < 0.001$ vs. Vehicle) and CRP ($p < 0.001$ vs. Vehicle) in the SP [500 $\mu\text{g}/\text{Kg}$] group (2) as a result of TLR4/NLRP3 pathway activation.

Conversely, the pre-treatment with pNAPE-LP/palmitate led to a parallel reduction in the release of IL-1 β ($p < 0.05$ vs. SP [500 $\mu\text{g}/\text{Kg}$]), IL-6 ($p < 0.01$ vs. SP [500 $\mu\text{g}/\text{Kg}$]), TNF α ($p < 0.01$ vs. SP [500 $\mu\text{g}/\text{Kg}$]) and CRP ($p < 0.001$ vs. SP [500 $\mu\text{g}/\text{Kg}$]), aligning with the down-regulation observed in the upstream proteins. In contrast, the pLP/palmitate (4) and Palmitate (5) groups did not exhibit such effects, as they displayed similar levels of IL-1 β , IL-6, and TNF α to those observed in the SP [500 $\mu\text{g}/\text{Kg}$] group (2) (Fig. 3, E-H).

pNAPE-LP mitigates hyperthermia in mice

Because of the pro-inflammatory markers overexpression, the mice from SP [500 $\mu\text{g}/\text{Kg}$] group (2) displayed an increased body temperature during the SP exposition ($p < 0.05$ vs. Vehicle). Again, the prophylactic pNAPE-LP/Palmitate treatment was able to mitigate the hyperthermia to physiological levels ($p < 0.05$ vs. SP [500 $\mu\text{g}/\text{Kg}$]).

Discussion

The present study highlights the remarkable potential of the probiotic system pNAPE-LP in counteracting lung inflammation triggered by SARS-CoV-2 SP. This exceptional probiotic effectively colonizes mice lungs and releases the anti-inflammatory compound PEA. Moreover, pNAPE-LP exhibits a protective effect on alveolar morphology, effectively reducing lung injury induced by SARS-CoV-2 SP. This is achieved by mitigating TLR4-mediated NLRP3 activation and global ACE2 expression in the lungs, while also reining in innate immune system over-activation.

The notion of harnessing probiotics as formidable allies in the battle against COVID-19 has gained momentum due to their remarkable ability to modulate the microbiota in hollow organs [37, 38]. This modulation, in turn, exerts a positive influence on immune responses [39], resulting in a potential reduction in systemic inflammation [40, 41]—a critical factor in severe COVID-19 cases. Specifically, when probiotics are administered intranasally, they have demonstrated the capacity to shape the composition of the respiratory microbiota [42], a pivotal player in determining immune responses [43]. These beneficial microbial agents fortify the respiratory tract's defense mechanisms, fostering a stronger and more balanced immune reaction to viral infections [44]. By promoting the production of short-chain fatty acids and anti-inflammatory molecules, they have the potential to play a crucial role in quelling the body's inflammatory storm, potentially alleviating the severity of COVID-19 [45, 46].

By integrating the inherent attributes of probiotic strains with the capacity of pNAPE-LP to release PEA on-site, our probiotic system accomplishes the objective of significantly enhancing the anti-inflammatory impact in comparison to the unmodified strain. The majority of PEA's anti-inflammatory characteristics stem from its ability in counteracting the NF- κ B signaling pathway via the activation of PPAR receptors, with a strong affinity for PPAR- α [47]. Additionally, PEA has the capability to hinder NF- κ B through a dual mechanism: direct interaction with NF- κ B p65 or the stimulation of NF- κ B inhibitors (I κ Bs) expression across diverse cell types [48]. In our model, the opposition to the NF- κ B signaling pathway was indirectly validated by the observation of diminished levels of upstream (TLR4) and downstream (NLRP3, ILs, etc.) signaling molecules. Through this pathway inhibition, pNAPE-LP effectively governs several genes linked to pro-inflammatory cytokine transcription, culminating in reduced release of IL-6 and TNF- α .

Furthermore, in alignment with our prior *in vitro* findings, a significant reduction in NLRP3 expression was demonstrated, consequently lowering inflammasome activation within the cohort subjected to pNAPE-LP and palmitate treatment. This data strongly suggests that pNAPE-LP might hold a pivotal role in the regulation of the inflammatory processes implicated in the initiation of ARDS. By curtailing NLRP3-dependent pathways, this probiotic systematically targets and downregulates downstream products, including IL-1 β , a significant mediator in ARDS pathogenesis [49] and a potential pharmacological target in the early phases of COVID-19 [50]. The inhibition of the NLRP3/caspase-1 pathway within lung tissue also stands to be crucial in preventing the initiation of pyroptosis [51]. Such prevention could be deemed strategic since, in numerous pathological conditions and models, extensive pyroptosis triggered by NLRP3/caspase-1 activation has been linked to heightened neutrophil recruitment [52, 53] (See Fig. 6).

This scenario was notably observed in our experimental model's group treated with SP, as evidenced by increased neutrophil count and heightened MPO activity. In contrast to resident tissue macrophages, neutrophils exhibit greater immunoreactivity [54], and their activation often results in intensified inflammation. Notably, an excessive recruitment of neutrophils has been reported in severe stages of COVID-19 [55, 56]. The mitigation of pyroptosis facilitated by pNAPE-LP pre-treatment was indirectly confirmed by the reduction in neutrophil count and MPO activity within lung samples.

Furthermore, specific probiotic strains, notably from the *Lactobacillus* family, have exhibited direct antiviral effects [57–59], displaying the capacity to impede viral replication. While the precise mechanisms demand further elucidation, probiotics from the *Lactobacillus* genus seem adept

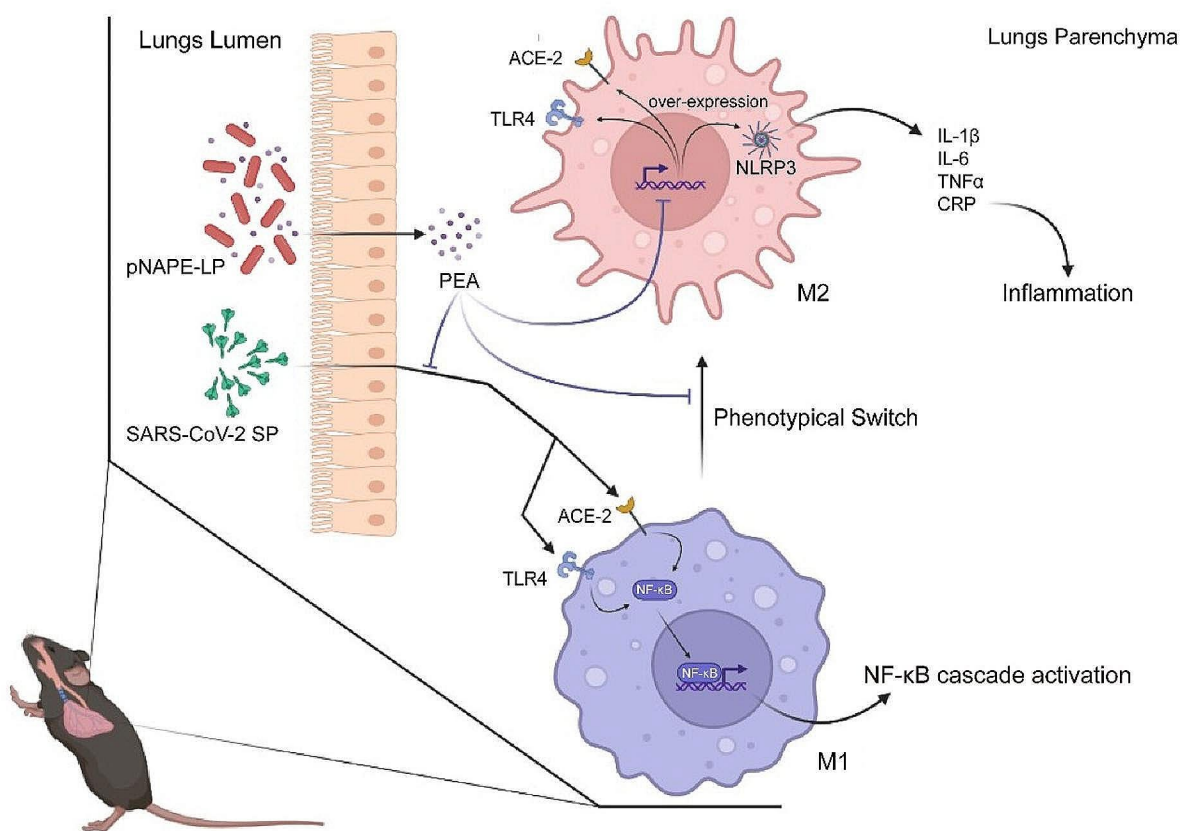


Fig. 6 Graphical representation of the main findings of the present paper

at lowering viral infection rates by establishing an antiviral state within macrophages [60, 61]. Within our probiotic system, this inherent antiviral activity of *Lactobacillus* strains harmonizes with PEA's ability to hinder SARS-CoV-2 infection by directly engaging with SP and ACE2 receptors [62], as well as its inhibitory influence on PPAR- α , which curbs viral replication [63]. Recent *in vitro* studies have indeed indicated that PEA's binding to the SARS-CoV-2 S protein results in approximately 70% reduction in viral infection among Huh-7 cells [62]. Furthermore, a previous research contribution from our team underscored SP's *in vitro* capability to elevate ACE2 receptor expression by instigating TLR4-mediated inflammatory responses [18]. Once again, this pattern was substantiated in our current *in vivo* study, evident in the ACE2/NLRP3 co-expression within lung tissues.

Scientific understanding dictates that proinflammatory elements, such as LPS (lipopolysaccharides) and/or pathological inflammatory states, are linked to elevated ACE-2 expression on tissue macrophages [19, 64]. Numerous investigations have indicated that elevated ACE expression in macrophages accentuates the immune response of these cells, potentially leading to a shift towards the M2 phenotype, indicating a regulatory role in the inflammatory process. It is plausible that SARS-CoV-2's SP potentially

fosters viral infection by enhancing ACE2 receptor expression in neighboring cells via the induction of inflammatory conditions in alveolar macrophages [18, 65]. However, the precise mechanism governing this ACE-2 upregulation by SP remains elusive and necessitates further exploration through additional studies. Conversely, our probiotic system effectively reversed the over-expression of ACE2 receptors, likely attributable to its anti-inflammatory impact. This intriguing effect holds the potential to mitigate the propagation of infection within lung tissue.

The findings presented in this study open up several avenues for future research and have significant implications for healthcare practices, particularly in the context of addressing lung inflammation triggered by SARS-CoV-2. Future research could focus on translating these findings into clinical trials to evaluate the safety and efficacy of pNAPE-LP in human subjects with SARS-CoV-2 infections. If proven effective, this probiotic system could be developed as a novel therapeutic strategy for managing COVID-19 and other respiratory infections. On the other hand, considering the complex nature of COVID-19 and its associated inflammatory responses, future investigation may also explore combination therapies. Combining pNAPE-LP with other anti-inflammatory agents or medications commonly used in COVID-19 treatment might enhance therapeutic outcomes.

This approach could be explored in preclinical models and, subsequently, in clinical trials.

Conclusion

In essence, the notion of harnessing probiotics as allies in the battle against COVID-19 is rapidly gaining traction. A number of studies have focused on the preclinical efficacy of recombinant probiotics as potential platform for oral and intranasal vaccines. The probiotic system, known as pNAPE-LP, has exhibited promising potential in addressing the lung inflammation triggered by SARS-CoV-2 SP, leading to a reduction in the excessive expression of the ACE2 receptor and a dampening of the inflammatory reaction. This holds the promise of yielding significant advantages in averting severe symptoms and secondary infections among COVID-19 patients, particularly within diverse demographics such as children and the elderly. Emphasizing the significance of localized PEA release is paramount. Notably, pNAPE-LP not only enhances the accessibility of PEA but also has the unique capability to selectively augment its presence precisely where it is required. This characteristic positions it as a novel and auspicious tool within the realm of precision medicine. Furthermore, the combination of immune-modulatory attributes inherent in a probiotic with the potent anti-inflammatory effects of PEA bestows upon pNAPE-LP a distinct superiority when compared to these two individual components in isolation.

In conclusion, the innovative synergy between probiotics and the pNAPE-LP system holds potential in reshaping our approach to combating COVID-19 and its associated inflammatory challenges.

Supplementary Information

The online version contains supplementary material available at <https://doi.org/10.1186/s41231-024-00167-x>.

Supplementary Material 1: Includes 2 Supplementary Tables: solutions for intranasal administration and volumes; Lung injury score assessment. Includes Supplementary Figure 1: effect of pNAPE-LP/Palmitate in healthy lung of mice.

Acknowledgements

Not applicable.

Author contributions

A.D.R. and G.E. (Giuseppe Esposito) conceptualize the experiment and the ideas in the paper; J.L. generate the engineered probiotic pNAPE-LP; A.D.R., S.B.F., I.P. and A.Z. performed the immunofluorescent analysis, the histological investigations and the ELISA tests; L.S. performed the western blot analysis; A.T. and F.P. performed the HPLC-MS; A.D.R. and G.E. (Giuseppe Esposito) wrote the manuscript; G.S., M.P. and G.E. (Giovanni Esposito) revised the manuscript; A.D.R. and G.E. (Giuseppe Esposito) supervised the project. All authors read and approved the final manuscript.

Funding

This research received no external fundings.

Data availability

All data generated or analysed during this study are included in this published article [and its supplementary information files].

Declarations

Ethics approval and consent to participate

The animal study protocol was approved by the Ethics Committee of Sapienza University of Rome (Organizzazione per il benessere animale, OPBA), approval code 890/2021-PR, approved on 17 November 2021. All animal experiments complied with the ARRIVE guidelines and were carried out in accordance with the U.K. Animals (Scientific Procedures) Act, 1986, and associated guidelines, E.U. Directive 2010/63/EU for animal experiments.

Consent for publication

Not applicable.

Competing interests

The authors declare that they have no competing interests. Giuseppe Esposito, Giovanni Esposito, Walter Sanseverino, and Giovanni Sarnelli are all affiliated with Nextbiomics s.r.l., Naples, Italy. Nextbiomics s.r.l. is an academic off-shoot of the University "Federico II" of Naples and should not, therefore, be perceived as a commercial conflict of interest.

Author details

¹Department of Physiology and Pharmacology "V. Erspamer", Sapienza University of Rome, Rome 00185, Italy

²Department of Anatomy and Cell Biology, China Medical University, Shenyang 110122, China

³Nextbiomics S.R.L. (Società a Responsabilità Limitata), Naples 80100, Italy

⁴Dipartimento di Chimica e Tecnologie del Farmaco, "Sapienza" University of Rome, P.le Aldo Moro 5, Rome 00185, Italy

⁵Department of Clinical Medicine and Surgery, Section of Gastroenterology, University Federico II, Naples 80138, Italy

⁶Department of Molecular Medicine and Medical Biotechnologies, Centro Ingegneria Genetica- Biotecnologie Avanzate, Naples 80131, Italy

Received: 26 December 2023 / Accepted: 29 February 2024

Published online: 20 March 2024

References

1. Marani M, Katul GG, Pan WK, Parolari AJ. Intensity and frequency of extreme novel epidemics. *Proc. Natl. Acad. Sci* 118, e2105482118 (2021).
2. WHO Coronavirus (COVID-19) Dashboard. <https://covid19.who.int>.
3. Lamers MM, Haagmans BL. SARS-CoV-2 pathogenesis. *Nat Rev Microbiol.* 2022;20:270–84.
4. Nesteruk I. Endemic characteristics of SARS-CoV-2 infection. *Sci Rep.* 2023;13:14841.
5. Baker RE, et al. Infectious disease in an era of global change. *Nat Rev Microbiol.* 2022;20:193–205.
6. Agrawal U, et al. Severe COVID-19 outcomes after full vaccination of primary schedule and initial boosters: pooled analysis of national prospective cohort studies of 30 million individuals in England, Northern Ireland, Scotland, and Wales. *Lancet.* 2022;400:1305–20.
7. Lee J-W, et al. The role of macrophages in the development of Acute and Chronic Inflammatory Lung diseases. *Cells.* 2021;10:897.
8. Budnevsky AV, et al. Role of mast cells in the pathogenesis of severe lung damage in COVID-19 patients. *Respir Res.* 2022;23:371.
9. McVey MJ, Steinberg BE, Goldenberg NM. Inflammasome activation in acute lung injury. *Am J Physiol - Lung Cell Mol Physiol.* 2021;320:L165–78.
10. Jo E-K, Kim JK, Shin D-M, Sasakawa C. Molecular mechanisms regulating NLRP3 inflammasome activation. *Cell Mol Immunol.* 2016;13:148–59.
11. van den Berg DF, te Velde AA. Severe COVID-19: NLRP3 Inflammasome Dysregulated. *Front Immunol.* 2020;11:1580.
12. Zhao C, Zhao W. NLRP3 Inflammasome—A key player in antiviral responses. *Front Immunol.* 2020;11:211.
13. Choudhury A, Mukherjee S. In silico studies on the comparative characterization of the interactions of SARS-CoV-2 spike glycoprotein with ACE-2 receptor homologs and human TLRs. *J Med Virol.* 2020;92:2105–13.

14. Brandão SCS, et al. Is toll-like receptor 4 involved in the severity of COVID-19 pathology in patients with cardiometabolic comorbidities? *Cytokine Growth Factor Rev.* 2021;58:102–10.
15. Zhao Y, et al. SARS-CoV-2 spike protein interacts with and activates TLR41. *Cell Res.* 2021;31:818–20.
16. SARS-CoV-2. drives NLRP3 inflammasome activation in human microglia through spike protein | *Molecular Psychiatry.* <https://www.nature.com/articles/s41380-022-01831-0>.
17. Yin M, Marrone L, Peace CG, O'Neill LA. J. NLRP3, the inflammasome and COVID-19 infection. *QJM Int J Med.* 2023;116:502–7.
18. Del Re A, et al. Ultramicronized Palmitoylethanolamide inhibits NLRP3 inflammasome expression and pro-inflammatory response activated by SARS-CoV-2 spike protein in cultured murine alveolar macrophages. *Metabolites.* 2021;11:592.
19. Veiras LC, et al. Over expression of ACE in myeloid cells increases immune effectiveness and leads to a new way of considering inflammation in acute and chronic diseases. *Curr Hypertens Rep.* 2020;22:4.
20. Khan Z, et al. Angiotensin-converting enzyme enhances the oxidative response and bactericidal activity of neutrophils. *Blood.* 2017;130:328–39.
21. Roncati L, Lusenti B, Pellati F, Corsi L. Micronized / ultramicronized palmitoylethanolamide (PEA) as natural neuroprotector against COVID-19 inflammation. *Prostaglandins Other Lipid Mediat.* 2021;154:106540.
22. Raciti L, De Luca R, Raciti G, Arcadi FA, Calabrò RS. The Use of Palmitoylethanolamide in the treatment of long COVID: a real-life Retrospective Cohort Study. *Med Sci.* 2022;10:37.
23. Pesce M, et al. Phytotherapies in COVID19: why palmitoylethanolamide? *Phytother Res.* 2021;35:2514–22.
24. Fessler SN, Liu L, Chang Y, Yip T, Johnston CS. Palmitoylethanolamide reduces proinflammatory markers in unvaccinated adults recently diagnosed with COVID-19: a Randomized Controlled Trial. *J Nutr.* 2022;152:2218–26.
25. Albanese M et al. Effects of Ultramicronized Palmitoylethanolamide (um-PEA) in COVID-19 Early Stages: A Case-Control Study. (2022).
26. Camerlingo C. Randomized clinical trial olfactory dysfunction after COVID-19: olfactory rehabilitation therapy vs. intervention treatment with Palmitoylethanolamide and Luteolin: preliminary results. *Eur Rev* <https://www.europe-anreview.org/article/26059> (2021).
27. Keppel Hesselink JM, de Boer T, Witkamp RF, Palmitoylethanolamide. A Natural Body-Owned Anti-Inflammatory Agent, Effective and Safe against Influenza and Common Cold. *Int. J. Inflamm* 2013, 151028 (2013).
28. Epitech Group SpA. *Efficacy of Palmitoylethanolamide, in add-on to Standard Therapy, on Inflammatory Markers of Patients With Interstitial Pneumonia Due to COVID-19. A Pilot Controlled, Randomized, Open Label Clinical Study.* <https://clinicaltrials.gov/study/NCT04568876> (2021).
29. Pharma FSD, Randomized IA., *Double-Blind, Placebo-Controlled, Multicenter Phase IIA Study of FSD201 (Ultramicronized PEA) + Standard of Care (SOC) Vs SOC in the Treatment of Hospitalized Patients With COVID-19.* <https://clinicaltrials.gov/study/NCT04619706> (2022).
30. Rankin L, Fowler CJ. The basal pharmacology of Palmitoylethanolamide. *Int J Mol Sci.* 2020;21:E7942.
31. Esposito G, et al. Engineered *Lactobacillus paracasei* producing Palmitoylethanolamide (PEA) prevents colitis in mice. *Int J Mol Sci.* 2021;22:2945.
32. Esposito G, et al. A palmitoylethanolamide producing *Lactobacillus paracasei* improves *Clostridium difficile* Toxin A-Induced Colitis. *Front Pharmacol.* 2021;12:639728.
33. Gopal G, Muralidar S, Kamalakkannan A, Ambi SV. Microbiome in Acute Respiratory Distress Syndrome (ARDS). in *Microbiome in Inflammatory Lung Diseases* (eds. Gupta, G., Oliver, B. G., Dua, K., Singh, A. & MacLoughlin, R.) 117–134 | Springer Nature, (2022). https://doi.org/10.1007/978-981-16-8957-4_8.
34. Kyo M, et al. Unique patterns of lower respiratory tract microbiota are associated with inflammation and hospital mortality in acute respiratory distress syndrome. *Respir Res.* 2019;20:246.
35. Ling LH, et al. Comparison of various tissue-Preparation techniques for Cryosectioning of Frozen Mouse tissues. *J Histotechnol.* 2009;32:186–9.
36. Paidi RK, et al. ACE-2-interacting domain of SARS-CoV-2 (AIDS) peptide suppresses inflammation to reduce fever and protect lungs and heart in mice: implications for COVID-19 therapy. *J Neuroimmune Pharmacol.* 2021;16:59–70.
37. Brahma S, Naik A, Lordan R. Probiotics. A gut response to the COVID-19 pandemic but what does the evidence show? *Clin Nutr Espen.* 2022;51:17–27.
38. Tian Y et al. Probiotics improve symptoms of patients with COVID-19 through gut-lung axis: a systematic review and meta-analysis. *Front Nutr* 10, (2023).
39. Mazziotta C, Tognon M, Martini F, Torreggiani E, Rotondo JC. Probiotics mechanism of action on Immune cells and Beneficial effects on Human Health. *Cells.* 2023;12:184.
40. Monteros MJM, et al. Probiotic lactobacilli as a promising strategy to ameliorate disorders associated with intestinal inflammation induced by a non-steroidal anti-inflammatory drug. *Sci Rep.* 2021;11:571.
41. Klaenhammer TR, Kleerebezem M, Kopp MV, Rescigno M. The impact of probiotics and prebiotics on the immune system. *Nat Rev Immunol.* 2012;12:728–34.
42. Wu Y, et al. Effect of probiotics on nasal and intestinal microbiota in people with high exposure to particulate matter $\leq 2.5 \mu\text{m}$ (PM_{2.5}): a randomized, double-blind, placebo-controlled clinical study. *Trials.* 2020;21:850.
43. Yuksel N, Gelmez B, Yildiz-Pekoz A. Lung microbiota: its relationship to Respiratory System diseases and approaches for Lung-targeted probiotic Bacteria delivery. *Mol Pharm.* 2023;20:3320–37.
44. Li Z, et al. Targeting the Pulmonary Microbiota to Fight against Respiratory diseases. *Cells.* 2022;11:916.
45. Machado MG, Sencio V, Trottein F. Short-chain fatty acids as a potential treatment for infections: a closer look at the lungs. *Infect Immun* 89, (2021).
46. Włodarczyk J, Czerwiński B, Fichna J. Short-chain fatty acids—microbiota cross-talk in the coronavirus disease (COVID-19). *Pharmacol Rep.* 2022;74:1198–207.
47. Lo Verme J, et al. The nuclear receptor peroxisome proliferator-activated receptor- α mediates the anti-inflammatory actions of palmitoylethanolamide. *Mol Pharmacol.* 2005;67:15–9.
48. Korbecki J, Bobiński R, Dutka M. Self-regulation of the inflammatory response by peroxisome proliferator-activated receptors. *Inflamm Res.* 2019;68:443–58.
49. Kolb M, Margetts PJ, Anthony DC, Pitossi F, Gaudie J. Transient expression of IL-1 β induces acute lung injury and chronic repair leading to pulmonary fibrosis. *J Clin Invest.* 2001;107:1529–36.
50. van de Veerdonk FL, Netea MG. Blocking IL-1 to prevent respiratory failure in COVID-19. *Crit Care.* 2020;24:445.
51. Yu P, et al. Pyroptosis: mechanisms and diseases. *Signal Transduct Target Ther.* 2021;6:1–21.
52. Chen L, et al. Neutrophil extracellular traps promote macrophage pyroptosis in sepsis. *Cell Death Dis.* 2018;9:1–12.
53. Liu L, Sun B. Neutrophil pyroptosis: new perspectives on sepsis. *Cell Mol Life Sci.* 2019;76:2031–42.
54. Yang S-C, Tsai Y-F, Pan Y-L, Hwang T-L. Understanding the role of neutrophils in acute respiratory distress syndrome. *Biomed J.* 2021;44:439–46.
55. Kuri-Cervantes L, et al. Comprehensive mapping of immune perturbations associated with severe COVID-19. *Sci Immunol.* 2020;5:eabd7114.
56. Ruan Q, Yang K, Wang W, Jiang L, Song J. Clinical predictors of mortality due to COVID-19 based on an analysis of data of 150 patients from Wuhan, China. *Intensive Care Med.* 2020;46:846–8.
57. Wang Y, Moon A, Huang J, Sun Y, Qiu H-J. Antiviral effects and underlying mechanisms of Probiotics as Promising antivirals. *Front Cell Infect Microbiol.* 2022;12:928050.
58. Salaris C et al. *Lactocaseibacillus Paracasei* DG enhances the lactoferrin anti-SARS-CoV-2 response in Caco-2 cells. *Gut Microbes* 13, 1961970.
59. Montazeri-Najafabady N, Kazemi K, Gholami A. Recent advances in antiviral effects of probiotics: potential mechanism study in prevention and treatment of SARS-CoV-2. *Biol (Basel).* 2022;77:3211–28.
60. Sundararaman A, Ray M, Ravindra PV, Halami PM. Role of probiotics to combat viral infections with emphasis on COVID-19. *Appl Microbiol Biotechnol.* 2020;104:8089–104.
61. Ivec M, et al. Interactions of macrophages with probiotic bacteria lead to increased antiviral response against vesicular stomatitis virus. *Antiviral Res.* 2007;75:266–74.
62. Fomesu R, et al. Palmitoylethanolamide (PEA) inhibits SARS-CoV-2 entry by interacting with S protein and ACE-2 receptor. *Viruses.* 2022;14:1080.
63. Fantazzoli M, Amoroso R, Ammazalorso APPAR. Ligands induce antiviral effects targeting perturbed lipid metabolism during SARS-CoV-2, HCV, and HCMV infection. *Biology.* 2022;11:114.
64. Song X, et al. Little to no expression of angiotensin-converting enzyme-2 on most human peripheral blood immune cells but highly expressed on tissue macrophages. *Cytom Part J Int Soc Anal Cytol.* 2023;103:136–45.

65. Aboudounya MM, Heads RJ. COVID-19 and Toll-Like Receptor 4 (TLR4): SARS-CoV-2 May Bind and Activate TLR4 to Increase ACE2 Expression, Facilitating Entry and Causing Hyperinflammation. *Mediators Inflamm* 2021, 8874339 (2021).

Publisher's Note

Springer Nature remains neutral with regard to jurisdictional claims in published maps and institutional affiliations.